



PERGAMON

Aerosol Science 33 (2002) 237–255

Journal of
Aerosol Science

www.elsevier.com/locate/jaerosci

Inhalability of large solid particles

Nola J. Kennedy*, William C. Hinds

*Department of Environmental Health Sciences, Center for Occupational and Environmental Health, UCLA
School of Public Health, 650 Charles E. Young Drive South, Los Angeles, CA 90095-1772, USA*

Received 30 August 2000; received in revised form 29 June 2001; accepted 29 June 2001

Abstract

Large particles (10–150 μm) with systemic toxicity pose a health risk if inhaled regardless of where they deposit. This research seeks to better define particle inhalability, the fraction of airborne particles that are inhaled as a function of particle size.

Measurements of inhalability were made for solid particles using a 1.6 \times 1.6 \times 5-m wind tunnel. Tunnel air velocities were 0.4, 1.0, and 1.6 m/s. A full-size, full-torso mannequin was used to collect dust entering either the mouth or nose for breathing at minute volumes of 14.2, 20.8, and 37.3 l. The mannequin either faced the oncoming wind or rotated slowly (0.06 rpm) during sample collection. At the test section, air velocity was uniform to within 10% and aerosol concentration was uniform to within 15% over the central 80% of the cross section.

Orientation-averaged inhalability for mouth breathing was higher than the inhalable particulate mass (IPM) sampling criterion for particles smaller than 35 μm and lower than the criterion for larger particles, leveling off at about 30% for particles >70 μm . Facing-the-wind mouth inhalability showed the same trend as the IPM sampling criterion, but the measured values were 25% higher. Wind velocity and breathing pattern had little effect on inhalability for the range of conditions examined here. Orientation-averaged inhalability for nose breathing dropped quickly with particle size reaching less than 10% at 60 μm . Facing-the-wind nose inhalability was slightly increased for particles smaller than 60 μm compared to orientation averaged inhalability for nose breathing. © 2001 Elsevier Science Ltd. All rights reserved.

Keywords: Inhalability; Large particles; IPM; Inhalable fraction

1. Introduction

The objective of particle size-selective sampling in the work environment is to provide an appropriate measure of health hazard associated with exposure to an airborne contaminant,

* Corresponding author. Tel.: +1-310-794-7687; fax: +1-310-794-2106.

E-mail address: okennedy@ucla.edu (N.J. Kennedy).

given knowledge of the physical and toxicological properties of the particles. After years of research and discussion, the early 1990s brought broad agreement on sampling criteria for the measurement of worker exposure to occupational aerosols. Definitions of three progressively finer aerosol size fractions for assessment of aerosol exposure have been published by the American Conference of Governmental Industrial Hygienists (ACGIH, 1999a), the International Standards Organization (ISO, 1995) and the Comité Européen de Normalisation (CEN, 1993). Responsible agencies in the US and countries in the European Economic Community have begun to incorporate particle size-selective sampling criteria into the setting of health-based occupational exposure limits.

The accepted aerosol fractions are inhalable particulate mass (IPM), thoracic particulate mass (TPM), and respirable particulate mass (RPM). This research focuses on the inhalable fraction, which is defined as the fraction of particles, as a function of aerodynamic diameter that are inhaled through the nose or mouth during breathing (ACGIH, 1999b). The basis for the IPM sampling criterion is a body of works presented by Ogden and Birkett (1977), Armbruster and Breuer (1982), and Vincent and Mark (1982). Together, these studies were used to develop a sampling criterion for the IPM that is described by

$$IF = 0.5(1 + \exp(-0.06d_a)) \quad d_a \leq 100 \mu\text{m}, \quad (1)$$

where IF is the inhalable fraction associated with d_a , the particle aerodynamic diameter in μm .

The IPM sampling criterion has not been applied to particles with aerodynamic diameters larger than 100 μm , because there have been no published data in this size range. The accepted criterion is also limited to wind velocities between 1 and 4 m/s. In general, the original studies found that breathing rate has little effect on inhalability for the range of conditions considered. The sampling criterion for IPM represents only mouth breathing that is orientation-averaged with respect to wind direction. Recent investigations, described below, provide information that can be used to better define the inhalable fraction of a given aerodynamic diameter.

Recognizing that workplace wind speeds can exceed 4 m/s, particularly in the outdoor environment, Vincent, Mark, Miller, Armbruster, and Ogden (1990) proposed the following definition for IF, which is an empirical modification of Eq. (1):

$$IF = 0.5(1 + \exp((-0.06d_a)) + 10^{-5}U^{-2.75} \exp(0.055d_a)), \quad (2)$$

where U is the wind velocity in m/s and d_a is in μm . The equation is limited to particles less than 100 μm and wind velocities in the range of 1–9 m/s. While higher wind speeds can occur in the work environment, it is much more likely, however, that the wind speed in an indoor workplace will be lower than 0.5 m/s (Baldwin & Maynard, 1998). Aitken, Baldwin, Beaumont, Kenny, and Maynard (1999) investigated particle inhalability at very low wind speed conditions, less than 0.1 m/s, and found that inhalability under such conditions is greater than that expected for wind speeds above 1.0 m/s. The effect appears to be related to breathing pattern and indicates an increase in inhalability with an increase in respiratory minute volume.

While the effect of wind speed on inhalability has been studied, several parameters that may influence inhalability remain largely uninvestigated. These include the effect of particle size

for aerodynamic diameters larger than 100 μm , nose breathing, and mannequin orientation with respect to wind direction. Empirical data for the range of conditions presented in this paper are limited. However, Erdal and Esmen (1995) provide estimates of large particle (25–200 μm) inhalability in their paper that explores mathematical modeling of aspiration efficiencies for the human head as an aerosol sampler.

Data for particles larger than 100 μm are limited primarily because of the difficulty associated with working with such large particles with their high losses due to settling and impaction. However, it is useful to evaluate inhalability for particles larger than 100 μm because it is likely that such particles can be inhaled. This need has been indicated by the studies used to develop the IPM sampling criterion and by consideration of a worker positioned downwind from a source of large particles. Prior to this investigation, there were no studies focused on defining inhalability for nose breathing. Mouth breathing is the default, or worst case, condition for inhalability studies because nose inhalability is anticipated to be lower than mouth inhalability. Regardless, an evaluation of nose inhalability offers information useful for both workers operating at low levels of work activity and for those who are using mouth breathing because even at high levels of work activity 50% of inhaled air is drawn through the nose (ICRP, 1994).

For the IPM sampling criterion, which is assumed to have orientation-averaged positioning with respect to wind direction, inhalability was based on studies that used arithmetic averaging of measurements from discrete angles to the oncoming wind. Measurements of the inhalable fraction that are sharply focused on the facing-the-wind direction may cause an overestimation of inhalability because of the high inhalability over the narrow range of angles around 0° with respect to wind direction and low inhalability elsewhere. This is consistent with the earlier data of Kuo (1993). Consequently, it is desirable to collect orientation-averaged measurements using a mannequin that rotates through 360° during sampling to ensure that the evaluation of inhalability is based on equal weighting of all sampling angles.

The primary aim of this research is to better define the sampling criterion for IPM by expanding current understanding of the inhalability of large particles. Inhalability is defined as the measured aspiration efficiency of the mouth or nose for a breathing, full-size, full-torso mannequin as a function of particle aerodynamic diameter. This study was designed to extend the particle size range to an aerodynamic diameter of 140 μm and to more completely examine the effects of wind velocity and breathing pattern on inhalability. It also investigates the difference between mouth and nose inhalability.

2. Experimental

To accomplish the above stated objectives, the effects of five variable parameters were evaluated:

2.1. Particle size

Nine particle sizes of aluminum oxide (Al_2O_3) dust were used. The mass median aerodynamic diameters (MMADs) were 7, 17, 22, 37, 52, 68, 82, 116, and 141 μm with

geometric standard deviations ranging from 1.13 to 1.36. These represent narrowly distributed, but not monodisperse, particles. Since inhalability changes relatively slowly with changes in aerodynamic diameter, the small changes in size that accompany use of a narrowly distributed test dust should not present a significant error.

Aluminum oxide particles are irregularly shaped and have a density of 3960 kg/m^3 . It was necessary to determine a scaling factor to allow calculation of aerodynamic diameter from measures of physical diameter. In addition, measuring aerodynamic settling velocity for individual particles using an illuminated settling tube was problematic. Particles that were large enough to isolate and manipulate, those with a physical diameter (d_p) larger than $70 \text{ }\mu\text{m}$, settled too quickly for manual timing. Particles small enough to settle slowly, $d_p < 40 \text{ }\mu\text{m}$, were too difficult to handle. The problem was addressed by measuring hydrodynamic settling velocity and then calculating aerodynamic diameter. The calculated aerodynamic diameter was compared to the measured physical diameter and a scaling factor was determined. Individual particles were isolated under $40\times$ power of an optical microscope and their shapes and physical diameters (d_p) were recorded.

Physical diameter was determined by comparing the projected-area diameter of each particle with calibrated, standard circles in a Porton graticule. Each circle in the progression represents a geometric increase in diameter (a doubling of area) over the previous circle; for example, the diameter of circle 7 is equal to the diameter of circle 6 multiplied by the square root of 2. The interval between two circles in the Porton graticule was further divided to refine sizing of the particles. Each sized particle was transferred to an illuminated vertical settling tube (a 100-ml graduated cylinder) filled with water and its travel time between two points was measured. There was no observable turbulence or convection during the descent of the particles. Water temperature was monitored during each measurement because it affects viscosity. This procedure was repeated for 51 particles with d_p between 70 and $110 \text{ }\mu\text{m}$ from a range of Al_2O_3 batches.

The measured hydrodynamic settling velocity was used to determine the diameter of a spherical particle, d_s , with the same hydrodynamic settling velocity, $V_{\text{TS,H}_2\text{O}}$.

$$d_s = \left(\frac{18\eta_{\text{H}_2\text{O}}V_{\text{TS,H}_2\text{O}}}{(\rho_p - \rho_{\text{H}_2\text{O}})g} \right)^{1/2}, \quad (3)$$

where $\eta_{\text{H}_2\text{O}}$ is the viscosity of water (see below), ρ_p is the density of the particle (3960 kg/m^3), $\rho_{\text{H}_2\text{O}}$ is the density of water (997.78 kg/m^3 at 22°C to 997.07 kg/m^3 at 25°C ; CRC, 1983), and g is the force of gravity (9.81 m/s^2).

Viscosity of water is highly dependent on water temperature. The value for viscosity of water at temperature $T(\eta_T)$ was calculated using the empirical equation

$$\log_{10} \frac{\eta_T}{\eta_{20}} = \frac{1.3272(20 - T) - 0.001053(T - 20)^2}{T + 105}, \quad (4)$$

where η_{20} is accepted to be $1.002 \times 10^{-3} \text{ Pa}\cdot\text{s}$ (CRC, 1983). Water viscosity ranged from $8.904 \times 10^{-4} \text{ Pa}\cdot\text{s}$ (25°C) to $9.548 \times 10^{-4} \text{ Pa}\cdot\text{s}$ (22°C).

Table 1
Aluminum oxide test dust particle size information

CMD ^a (μm)	CMAD ^b (μm)	GSD ^a	MMAD ^c (μm)
4.4	6.2	1.27	7
9.2	12.9	1.36	17
14	19.6	1.21	22
20	28.0	1.35	37
29	40.6	1.34	52
41	57.4	1.27	68
55	77.0	1.16	82
75	105.0	1.20	116
96	134.4	1.13	141

^aDetermined by optical microscopy.

^bCMAD = CMD × scaling factor (1.4).

^cMMAD = CMAD exp(3 ln² GSD).

The 51 particles that were evaluated each had a Reynold's number when settling in air, Re_{air} , greater than 0.5 (0.62–10.46), which is outside the Stoke's region and makes calculation of $V_{TS,air}$ and d_a more difficult. The difficulty arises because of a shift in the relationship between particle settling velocity and particle size from $V_{TS} \propto d_a^2$ to $V_{TS} \propto d_a^{1/2}$. Aerodynamic diameters were calculated using empirical equations given by Hinds (1999) for particle motion with $0.5 < Re < 100$.

The calculated values of aerodynamic diameter were compared to the physical diameters and the average ratio served as a scaling factor. The scaling factor for particles with d_p in the range of 70–110 μm was 1.4. This scaling factor is related to, but not the same as, a dynamic shape factor because the particles we evaluated were outside the Stoke's region. The scaling factor was assumed to hold for smaller particles. This assumption is supported by size measurements made using an Aerosizer time-of-flight instrument (Amherst Process Instruments, Hadley, MA). The Aerosizer gave relative data that was linear over the entire range of particle sizes included in the study; this allowed confidence that the scaling factor was linear for CMD vs. d_a . Mark, Vincent, Gibson, and Witherspoon (1985) used a sedigraph to determine the dynamic shape factor for Al₂O₃ particles ($6 \mu\text{m} < d_a < 90 \mu\text{m}$) and found that it ranged from 1.00 to 1.49 and was dependent on particle size. Table 1 lists the sizing information for the test particles.

2.2. Wind velocity

Three wind velocities were investigated: 0.4, 1.0 and 1.6 m/s. These are in the range that is generally considered typical for indoor work environments, although studies mentioned earlier indicate that these are at the high end for most workplaces. Early studies of inhalability found that the effect of wind velocity, for the range covered by this investigation, is weak compared to the effect of particle size. By evaluating the effect of wind velocity, this study sought to confirm previous findings.

Table 2

Work rate, respiration rate, minute volume and tidal volume for the selected breathing patterns

Work rate		Respiration rate (min ⁻¹)	Minute volume (l)	Tidal volume (l)
(W)	(kg m/min)			
0	0	19.6	14.2	0.72
35	208	21.2	20.8	0.98
105	622	23.0	37.3	1.62

2.3. Breathing pattern

The tests were conducted using three experimentally determined breathing pattern profiles associated with “rest”, “moderate”, and “heavy” work conditions (Silverman, Plotkin, Sawyers, & Yancey, 1951). Three inspiratory minute volumes were used: 14.2, 20.8 and 37.3 liters, which correspond to work rates of 0, 35, and 105 W (0, 208, and 622 kg m/min). Table 2 shows the minute volume, respiration rate, work rate and tidal volume for each of the three conditions. Once again, the results of this study can be used to confirm those of previous works that found little effect on inhalability related to breathing pattern.

2.4. Mannequin orientation

The position of the mannequin with respect to the oncoming wind is expected to have considerable effect on large particle inhalability with greater efficiency occurring in a narrow range of angles around 0° (facing-the-wind). This study investigated two orientations with respect to the oncoming wind: facing-the-wind and orientation averaged. The facing-the-wind condition provides the upper limit for inhalability and the orientation-averaged condition, by equally weighting the aspiration efficiencies associated with all angles from 0° to 360°, is representative of typical exposures when there is no dominant wind direction. The mannequin completes one full rotation, always in the same direction, during each orientation-averaged sampling run. Sampling duration for each condition was long enough to ensure adequate dust collection for gravimetric analysis.

2.5. Mouth vs. nose breathing

It is easy to imagine that the open mouth, with its larger area and axial orientation, will collect large particles more efficiently than the nostrils. This is complicated by the flow of air around and near the torso and head. Airstreams approaching the torso must diverge and compress to allow the air to get past the obstruction. This results in lateral, vertical and horizontal motion of the air. In the immediate vicinity of the mouth or nose the streamlines converge to enter the mouth or nose. Turbulence and eddies form and the airflow and movement of aerosol particles becomes difficult to predict. As mentioned earlier, initial investigations into the modeling of inhalability have been conducted (Erdal & Esmen, 1995).

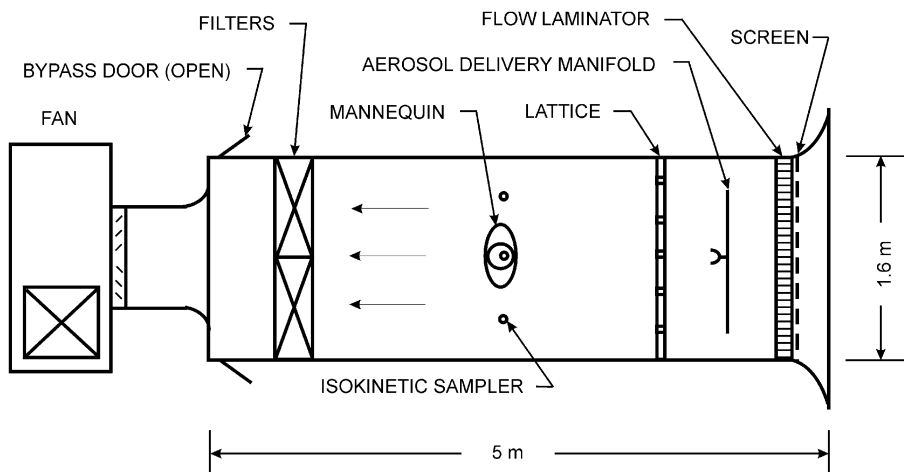


Fig. 1. Diagram of the wind tunnel.

Workers at low activity tend to breathe through their nose. As activity level increases, workers begin to also breathe through their mouth. This investigation compares 100% nose and 100% mouth breathing at one work rate and one wind velocity. The goal is to determine the difference in inhalability due to exclusive mouth or nose breathing.

2.6. Test system

There are three primary components of the experimental test system: (1) the wind tunnel, (2) the mannequin and breathing machine, and (3) the dust generation system.

Wind tunnel. It is widely accepted that a large-scale, low-velocity wind tunnel is required for studies of particle inhalability. Airflow around the complex geometry of the nose and mouth is influenced by the presence of the body, dictating a requirement to use a full-size mannequin (Vincent, 1989). To minimize distortion of airflow in the wind tunnel a large cross-sectional area is necessary. The UCLA Low-Velocity Wind Tunnel (Hinds & Kuo, 1995) was used during this investigation. This wind tunnel has a 1.6 m × 1.6 m cross section, accommodates a full-size mannequin, and is capable of wind speeds in the range of 0.1–2.0 m/s. A diagram of the wind tunnel is presented in Fig. 1. The mannequin blocks between 4% and 11% of the cross-sectional area of the wind tunnel, depending on which direction it faces.

Mannequin and breathing machine. A full-size, full-torso fiberglass mannequin (Model SM701, Silvestri Co., Los Angeles, CA) was used for the study. The face size represents overlapping dimensions for men and women (Douglas, 1991). The facial dimensions are 22.5 cm long by 13.4 cm wide. The mouth opening is a 30 mm × 6 mm oval with an area of 1.6 cm². The mouth sampler inlet was shaped from 20-mm ID copper tubing and is connected to an aluminum 47-mm filter holder. The path length from the mouth inlet to the filter is 62 mm. The nasal openings are 7 mm × 10 mm ovals and the nose sampler uses two 6-mm ID brass tubes connected to a single 16-mm ID copper tube that is attached to a 47-mm filter holder.

The path length from the nasal inlets to the filter is 95 mm. The back of the mannequin's head is removable to allow insertion of 47-mm filter holders within the cavity. A diagram of the mannequin head and the filter holder placement is provided by Hinds and Kuo (1995). The back of the head is replaced and a wig is fitted on the mannequin during sampling. The mannequin is coated with conductive paint (EMI/RFI Shield Coat, distributed by McMaster-Carr, Santa Fe Springs, CA) and its surface grounded.

A cam-driven mechanical breathing machine (Nelson, Johnson, Lindeken, & Taylor, 1972) simulated the selected breathing patterns. Two hoses, one for inhalation and one for exhalation, connected the nose or mouth sampler through direction-control valves to the breathing machine. Previous studies of inhalability have used cyclic sampler flow to simulate human breathing; however, this study was designed to allow exhalation back through the mouth or nose. Consider the exhaled breath of a worker exposed to large particles and facing the wind. Inhaled particles are removed by deposition mechanisms and a jet of clean air is exhaled into the flow field around the mouth or nose just prior to the next inhalation. Airflow near the sampler (mouth or nose) is changed and mixing with the clean exhaled air, which will alter the aerosol concentration in the vicinity of the sampler, could affect measurements of inhalability. Consequently, exhalation back through the sampler is included in these experiments. Although the exhaled air is delivered in front of the filter to prevent interference with the sample, there was some concern that exhaled air might dislodge collected particles from the filter and sampler inlets. An evaluation of sample loss due to exhalation indicated negligible loss of particles from the filter or inlet.

Dust generation. Narrowly graded aluminum oxide (Al_2O_3) optical powder (General Abrasives/Treibacher, Inc., Niagara Falls, NY) was used as the test dust. In some cases, the bulk material was used as received, but most of the dusts were either sieved using USA standard test sieves (Fisher Scientific Co., USA) and a Gilson sieve shaker, model SS8-R (Gilson Co., Inc., Worthington, OH) or separated using a centripetal classifier (Vortec Products Co., Long Beach, CA). The dust was dispersed using three NBS-type (BGI, Inc., Waltham, MA) dust feeders (Hinds, 1999) mounted on top of the wind tunnel. Average dust concentrations in the wind tunnel test section were between 100 and 300 mg/m^3 with less than 15% spatial variation over the central 80% of the test section. This was tested using horizontal and vertical 11-point traverses. The temporal variation in wind velocity in the wind tunnel is less than 10% (Kuo, 1993).

The Al_2O_3 particles were found to carry an extremely high level of charge, +240.00 charges on particles with a physical diameter of 30 μm . The measured high charge levels and the extremely high resistivity of Al_2O_3 , $10^{14} \Omega\text{m}$ (CRC, 1983), along with the observed build up of unneutralized particles in the test system, precipitated the acknowledgement that particle charge could affect measurements of inhalability. This made it necessary to ground all components of the wind tunnel and develop a system to reduce particle charge (Hinds & Kennedy, 2000). The neutralization device, an asymmetrical 5-electrode ion generator, did not reduce the charge distribution level to Boltzmann's equilibrium, but it did provide charge levels within the range expected for typical workplace aerosols (Vincent, Johnston, & Jones, 1984). This was necessary to minimize the effect of electrostatic charge on measurements of inhalability.

2.7. Test strategy

With three replications for each set of conditions, there were 36 experimental runs for each of nine particle sizes giving a minimum of 324 runs. For each particle size and breathing rate the runs were sequenced randomly. After the initial runs were completed, unreliable data were discarded and the runs repeated. Runs were repeated when there was experimental error due to malfunction of mechanical equipment or operational mistakes or when systematic error was indicated by a data set with a coefficient of variation >0.3 . The coefficients of variation ranged from 0.009 to 0.853 with an average of 0.106. New data were averaged with the initial data to determine inhalability.

Inhalability was calculated as the ratio of the mass concentration “inhaled” by the mannequin to the average mass concentration measured by the three isokinetic samplers placed 0.3 m to each side and above the mouth of the mannequin. The isokinetic sampler locations had previously been determined to be the closest location to the mannequin’s mouth for which the presence or absence of the mannequin had no effect on air velocity, direction, or measured concentration (Hinds & Kuo, 1995). It was assumed that uniformity of aerosol concentration in the test section was maintained when the mannequin was in place. Fig. 2 shows the mannequin and location of the isokinetic samplers. The isokinetic samplers are constructed from 25-mm in-line stainless-steel filter holders (Gelman Sciences, Inc., Ann Arbor, MI, P/N 1209) fitted with 8.5-mm ID brass probes that extend 32 mm from the face of the holder. The probes were filed to form a sharp edge at the inlet.

All samples were collected on glass fiber filters cut from Whatman EPM 2000 filter paper sheets (Whatman International Ltd., Maidstone, England). Care was taken to ensure that all particles penetrating the plane of each sampler inlet were included in the sample. Using fine-bristled artist’s brushes, particles that settled on the interior walls of the sampler and filter holder were gently brushed onto the filter prior to weighing. A calibrated Cahn C-35 microbalance (Orion Research, Inc., Boston, MA) with a precision of 0.01 mg was used to weigh the filters before and after sampling. For larger particles ($d_a > 68 \mu\text{m}$) only the two side isokinetic samplers were used to determine wind tunnel mass concentration because the aerosol sampled by the top isokinetic sampler was not representative of the aerosol concentration in the vicinity of the mouth or nose due to settling. For the largest particles (141 μm) and the lowest wind velocity (0.4 m/s) sampling was not possible because nearly all particles had settled below the level of the samplers.

3. Results and discussion

3.1. Orientation-averaged mouth inhalability

The combined results, including all wind speeds and breathing patterns, for orientation-averaged mouth inhalability are shown in Fig. 3. Also shown is the accepted IPM sampling criterion curve. The data show a similar shape to the criterion curve for IPM sampling, but exhibit lower inhalability for particles larger than 35 μm . While the criterion curve plateaus at an inhalability of about 50% for particles larger than 50 μm , the data indicate a plateau at about



Fig. 2. Mannequin and isokinetic samplers.

30% for particles larger than $75 \mu\text{m}$. The data from this study are similar to results published from an investigation of large particle and wall deposition effects in inhalable samplers (Aitken & Donaldson, 1996). The following empirical equation describes the curve obtained from the measurements of the inhalable fraction (IF_M) for orientation-averaged mouth breathing:

$$\text{IF}_M = 24.14 + 75.86 \exp(-0.00607d_a^{1.400}). \quad (5)$$

This equation is valid for particles up to $141 \mu\text{m}$, wind velocities in the range of $0.4\text{--}1.6 \text{ m/s}$, and orientation-averaged mouth breathing with respiratory minute volumes between 14.2 and 37.3 l .

The reason for the difference between the data and the IPM sampling criterion is not evident, but there are some possible explanations. One factor is the difference in the methods used to determine orientation-averaged inhalability. A continuously rotating mannequin, as the one used in this investigation, provides a sample that is equally representative of all angles. Prior

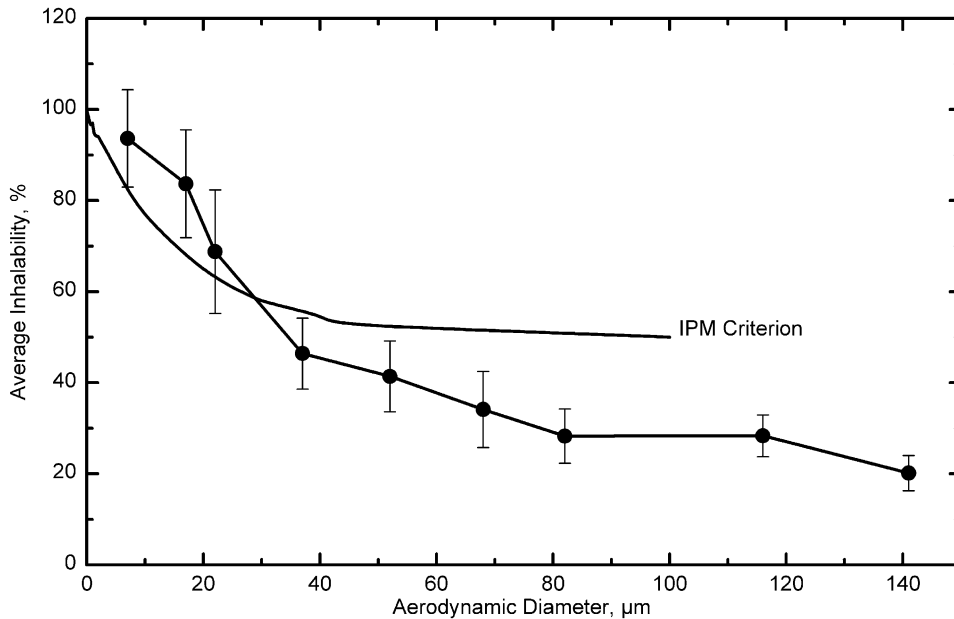


Fig. 3. Inhalability for orientation-averaged mouth breathing, combined results.

studies determined orientation-averaged inhalability as the simple average of results obtained from measurements at discrete angles, such as, 0° , 45° , 90° , etc. Since aspiration efficiency is much greater when the sampler is oriented in a narrow range of angles around 0° , the use of discrete angles may overestimate the contribution of the facing-the-wind condition. This would result in a higher value for large particle inhalability.

Another explanation is that previous studies did not neutralize the charge on the test particles. Vincent and Mark (1982) noted the accumulation of dust around the mouth of their mannequin. The dust could have been dislodged by incoming particles, inhaled, and included in their samples. This would, in effect, increase the observed values for inhalability. To minimize this effect, they greased the mouth and nose of their mannequin. Since charged particles could have affected the results, care was taken during this work to ground all components of the test system and neutralize the charge on particles. During these experiments, the mannequin face was periodically wiped clean and accumulations of dust around the nose and mouth were not observed.

A third possibility is the difference in the breathing mechanism of the mannequins. Mannequins used in previous studies inhaled through the mouth and the exhaled air exited either through the back of the head or through the nostrils. The mannequin used in this study inhaled and exhaled through the same path; air inhaled through the mouth was exhaled through the mouth and air inhaled through the nose was exhaled through the nose. The exhalation of clean air may create a region in front of the sampler (mouth or nose) where the aerosol concentration is low. This could result in lower values for inhalability for the measurements reported here.

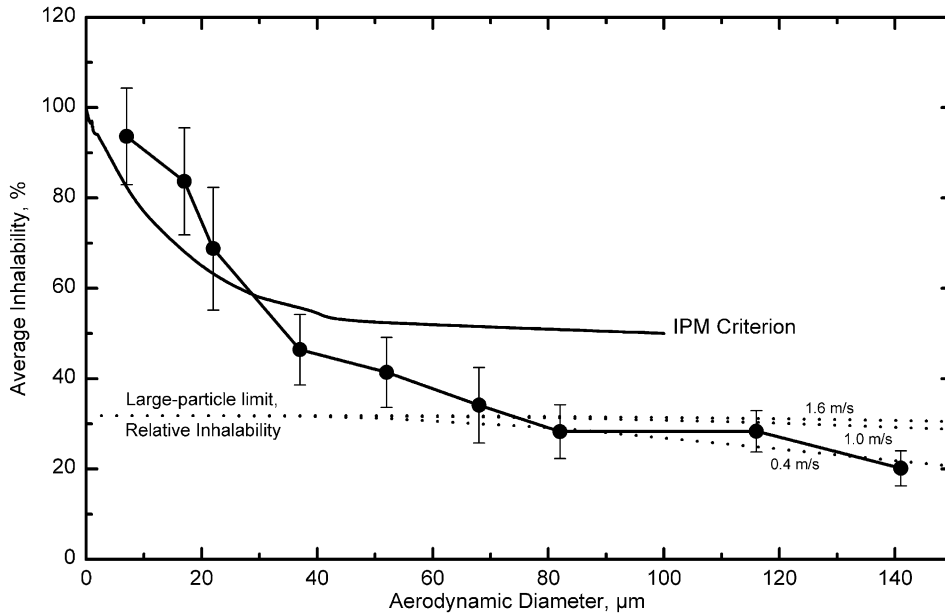


Fig. 4. Theoretical large-particle limits for relative inhalability.

The fourth possibility is general and speaks to the notion that wind tunnel test systems for inhalability are complex and unique. Considering the specialized set up for individual test facilities, apparatus-specific variation may translate to differences in results. Comparisons were made between this system and those used by others. Several differences were noted, but none could be isolated as the cause of differences in results.

Fig. 4 shows lines (dashed) indicating the theoretical large-particle limit of relative inhalability for the three wind velocities for particles larger than 50 μm . The lines were developed based on two assumptions. First, large particles approaching the mannequin have sufficient inertia that they continue as projectiles in a straight line. That is, their original velocity, along the wind tunnel axis, is unaffected by aerodynamic forces or curving streamlines in the vicinity of the mannequin. Second, inhalability when the mannequin is facing the wind under these conditions is 100%. If particle settling is neglected, the inhaled concentration, C_I , is

$$C_I = \frac{\text{mass inhaled}}{\text{volume inhaled}} = \frac{C_m \times U \times A \cos \theta}{Q}, \quad (6)$$

where C_m is the mass concentration, U the wind tunnel air velocity, A the mouth area, Q the sampler flow rate, and θ the angle of the sampler (mouth) axis with respect to the oncoming wind. The $\cos \theta$ term is 1.0 for facing the wind and decreases to 0 at 90° to the wind. The relative inhalability, IF_{rel} , is the ratio of the inhaled concentration relative to that of the facing-the-wind condition. For continuous rotation

$$\text{IF}_{\text{rel}} = \frac{1/\pi \int_0^{\pi/2} C_I(\theta) d\theta}{C_I(\theta = 0^\circ)}, \quad (7)$$

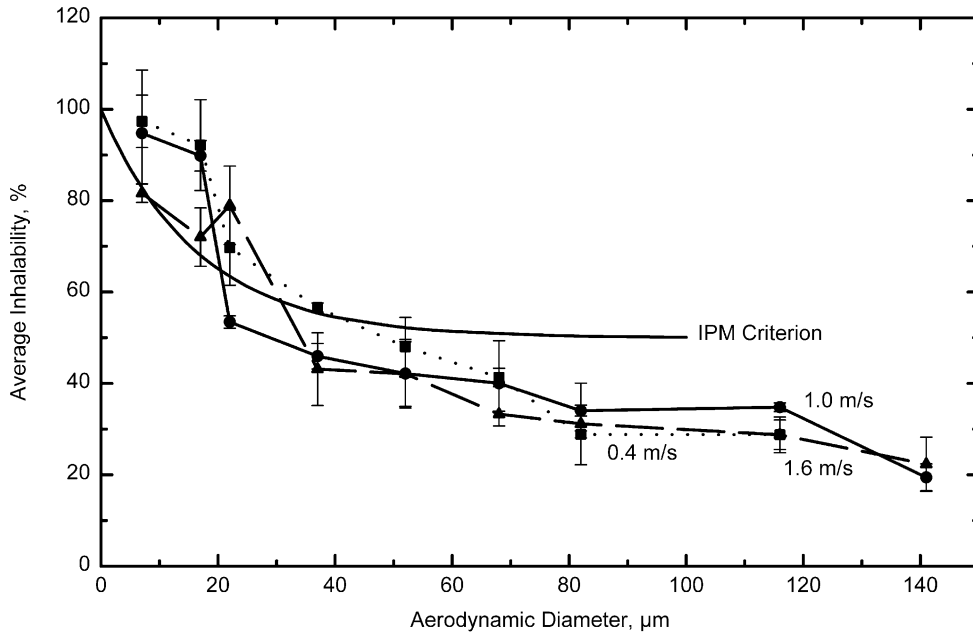


Fig. 5. Effect of wind velocity on orientation-averaged mouth inhalability.

where IF_{rel} is 0 when $\theta \geq \pi/2$. In Eq. (7) breathing-cycle flow rate cancels out so relative inhalability depends only on geometric factors.

For the largest particles at the lowest air velocities, the particles do not travel horizontally, so the inhaled concentration must be reduced by $\cos \phi$, where ϕ is the downward angle of the particle's straight-line trajectory resulting from settling,

$$\phi = \arctan\left(\frac{V_{TS}}{U}\right). \tag{8}$$

Mouth inhalability results show good agreement with the theoretical large particle limits for relative inhalability for $d_a > 60 \mu\text{m}$.

The results for the effect of wind velocity on orientation-averaged mouth inhalability are presented in Fig. 5. The data shown were collected at a respiratory minute volume of 20.8 liters. The three curves are similar in shape and follow the same general trend.

Appearance suggests that there is no effect related to wind velocity and statistical analysis confirms this decision. The data set passed tests for normal variance and equal variance, which allowed the use of a two-way analysis of variance (ANOVA). The difference between the mean values for the nine particle sizes was barely significant with $p = 0.0469$. This finding agrees with previous studies, which concluded that wind velocities in the range of 1–4 m/s have little effect on orientation-averaged mouth inhalability.

The effect of breathing pattern on orientation-averaged mouth inhalability is shown in Fig. 6. The data presented are for a wind velocity of 1.0 m/s. The curves are similar in shape and there is no clear systematic pattern. A two-way ANOVA finds that the variance due to changes in

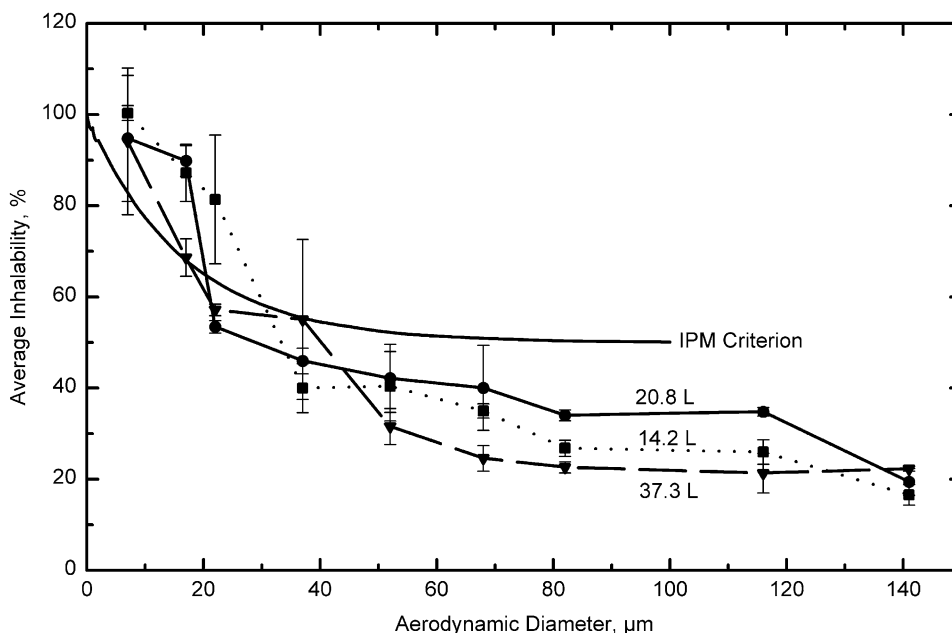


Fig. 6. Effect of breathing pattern on orientation-averaged mouth inhalability.

breathing rate is significant ($p=0.00213$) and that there is little interaction between breathing rate and particle size ($p=0.0405$). When comparing two curves at a time ($p<0.05$), those for minute volumes of 14.2 and 20.8 were not different, while those for 14.2 vs. 37.3 and 20.8 vs. 37.3 were different. Work by Ogden and Birkett (1977) found that the effect of breathing pattern was small and not particularly systematic; the data from this study confirm their finding. It is interesting to note that the mid-range breathing rate resulted in the highest inhalability. Possibly, this is the result of differences in airflow pattern in the region near the mouth associated with variation in breathing rate.

3.2. Facing-the-wind mouth breathing

Fig. 7 shows the combined data, including all wind velocities and breathing patterns, for facing-the-wind inhalability for mouth breathing. Inhalability plateaus at about 75% for particles between 20 and 115 μm and drops sharply to 50% for 140- μm particles. There are no previous studies for comparison and this represents the first evaluation of facing-the-wind inhalability for mouth breathing. For certain occupational environments this may be an important distinction. Large particle inhalability for workers facing into the oncoming wind is expected to be significantly higher than for workers exposed to omnidirectional airflow.

The data for the effect of wind velocity on facing-the-wind mouth inhalability are illustrated in Fig. 8. Again, the respiratory minute volume was 20.8 l/min. For particles larger than 70 μm , measured inhalability was greater with increased wind velocity. The results might be due to the competition between straight-line motion and settling for large particles. The effect appears

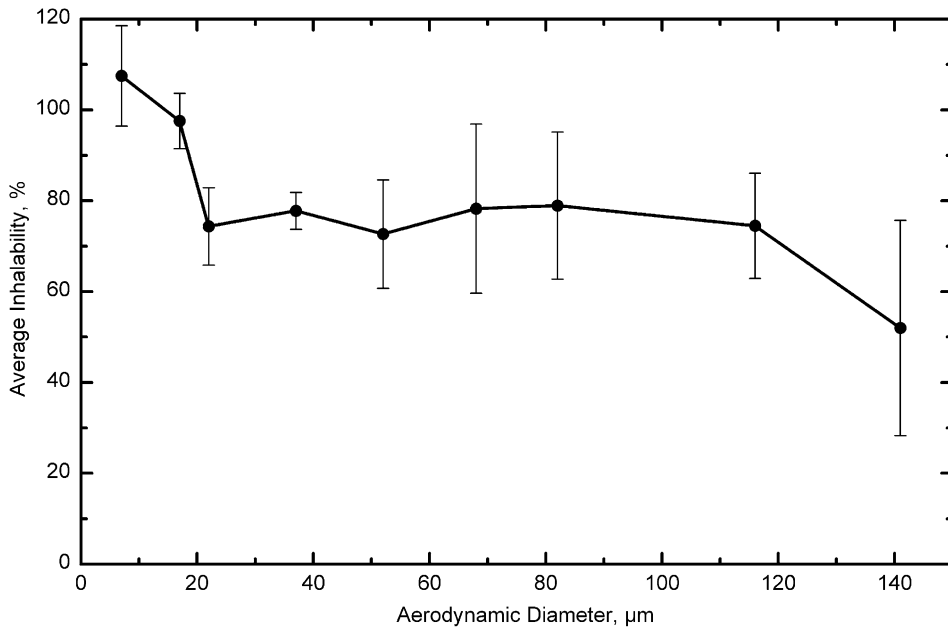


Fig. 7. Inhalability for facing-the-wind mouth breathing, combined results.

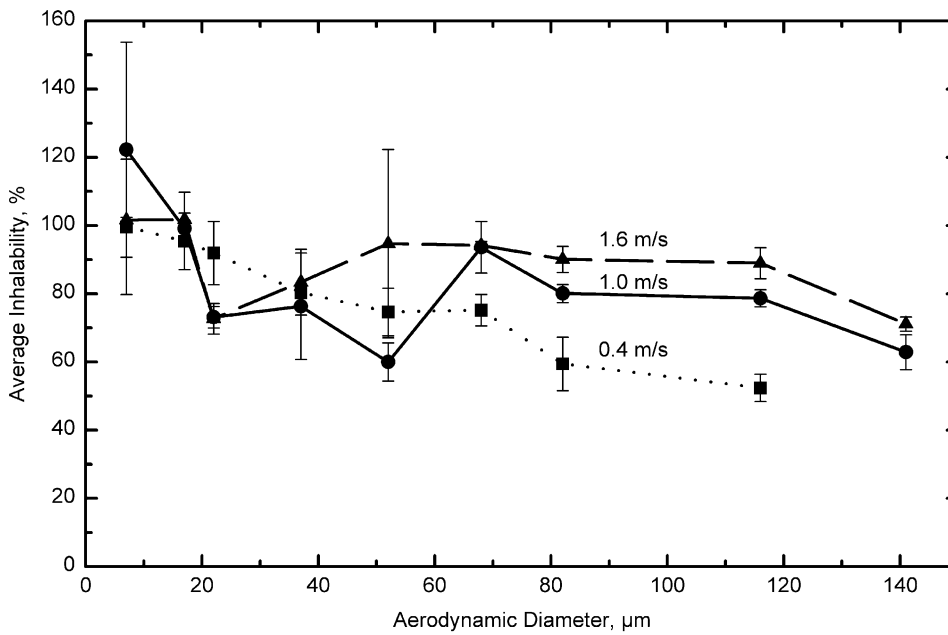


Fig. 8. Effect of wind velocity on facing-the-wind mouth inhalability.

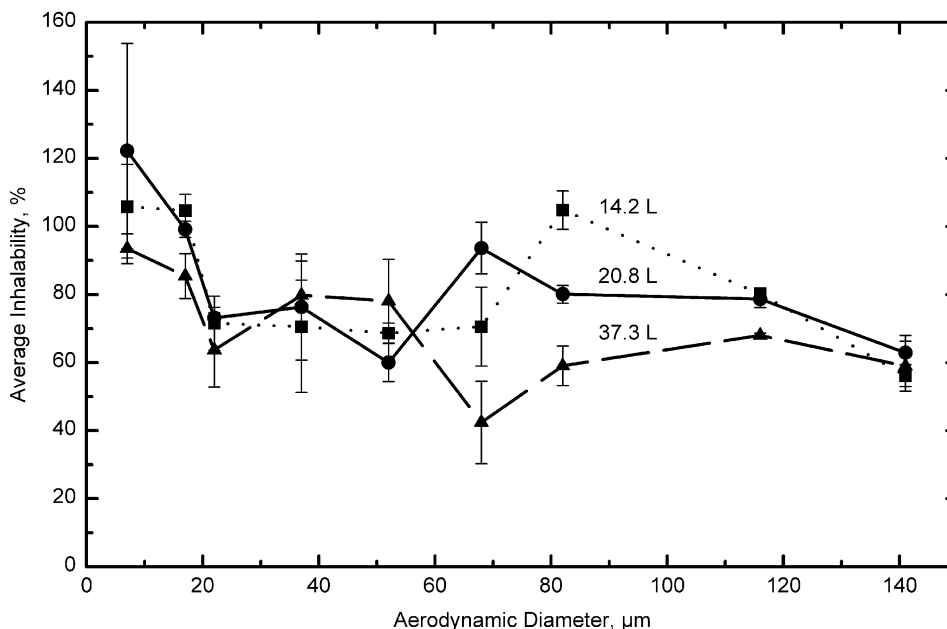


Fig. 9. Effect of breathing pattern on facing-the-wind mouth inhalability.

to be systematic and a two-way ANOVA found a significant difference due to wind velocity ($p=0.00440$), although a comparison of just two curves at a time ($p<0.05$) found significant variation between the lowest and highest wind velocity only.

Fig. 9 shows the effect of breathing pattern on mouth inhalability for facing-the-wind conditions. Wind velocity was 1.0 m/s for all samples. In general, the results show no clear pattern and it is difficult to see any relationship between breathing pattern and inhalability. A closer look suggests that there may be some systematic effect for particles larger than 80 μm . A two-way ANOVA indicates that the effect of breathing rate is significant ($p=0.0000925$) and that there is an interaction between breathing rate and particle size ($p=0.00225$). Once again, this is the first study that attempts to evaluate the effect of breathing pattern for facing-the-wind conditions and there are no other investigations available for comparison.

3.3. Nose breathing

Inhalability for orientation-averaged and facing-the-wind nose breathing is illustrated in Fig. 10. Orientation-averaged nose inhalability drops quickly from more than 60% for particles smaller than 20 μm to a plateau at less than 10% for larger particles. Facing-the-wind nose inhalability drops from nearly 100% for 7- μm particles to less than 10% for particles between 50 and 80 μm . For particles larger than 80 μm , there appears to be an increase in facing-the-wind nose inhalability, but the trend is not clear because of the large variability in the results for $d_a=116 \mu\text{m}$. The following empirical equation describes the curve obtained from the measurements of the inhalable fraction (IF_N) for orientation-averaged nose breathing

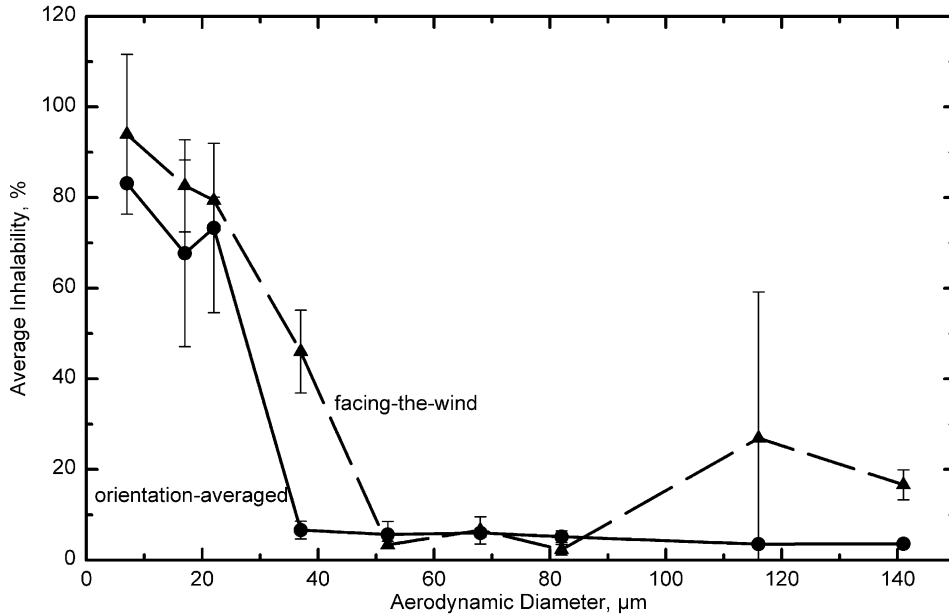


Fig. 10. Inhalability for nose breathing, orientation-averaged and facing-the-wind.

(Hinds, 1999):

$$IF_N = 0.035 + 0.965 \exp(-0.000113d_a^{2.74}). \quad (9)$$

For the range of particle sizes included in this study, inhalability for nose breathing does not appear to go to zero. This can be explained by the vertical motion of air, from the torso up toward the face, which can carry particles into the vicinity of the nose. This was the first comprehensive study of nose inhalability and there are no published data for comparison.

4. Conclusion

In general, wind velocities in the range of 0.4–1.6 m/s and breathing patterns associated with minute volumes of 14.2–37.3 l show little or no effect on measured mouth inhalability. Orientation with respect to wind direction has the greatest effect on inhalability and should be considered in reference to worker exposure monitoring. Facing-the-wind mouth inhalability is nearly twice that of orientation-averaged mouth inhalability measurements for particles larger than 40 μm. This is an important difference for workers who face the oncoming wind and are exposed to large particles. It means that their exposure to particles larger than 40 μm could be double the value predicted by a sampler designed to match an orientation-averaged curve, like the current sampling criterion for inhalable particulates.

The inhalability curve generated by our data shows a significant deviation from the IPM sampling criterion. The source of the difference is unknown, but may be related to differences in experimental set up. The investigators took care to minimize sampling errors and have

confidence in the data. Additionally, the curve has been extended beyond 100–140 μm . The results suggest that a revision of the current ACGIH/CEN/ISO IPM sampling criterion should be considered to account for differences in inhalability due to orientation with respect to wind direction, nose breathing, and to include particles larger than 100 μm .

A common trend in all of the curves for mouth inhalability is the consistent decrease in inhalability for particles larger than 116 μm . Certainly, the loss is related to aerodynamic behavior of the particles. It may be related to a complicated interaction between particle physics and air motion in the region of the mouth. Possibly, it is a result of the competition between horizontal velocity and settling velocity. It is an interesting trend and warrants further investigation.

The inhalability curve for nose breathing is notably different than the IPM sampling criterion. Personal sampling devices designed to meet the IPM sampling curve will overestimate the exposure contribution of particles larger than 30 μm . While this is unlikely to result in overexposure to toxic aerosols, it may not provide an accurate representation of exposure, especially for nose-breathing workers.

Acknowledgements

This study was supported by NIOSH research grant number 5-RO1/OH03196 and NIOSH Education and Research Center grant number T42/CCT910430. The authors wish to acknowledge the contributions of Jinghui Wang Zhang and Karina Tatyán, who were instrumental during data collection and the work of Ti-Lin Kuo in developing the test system and making preliminary measurements of inhalability. Sincere appreciation is also extended to Joe Bohan and the staff at Amherst Process Instruments (API) in Hadley, MA for their assistance in sizing the particles.

References

- Aitken, R. J., & Donaldson, R. (1996). *Large particle and wall deposition effects in inhalable samplers*. HSE Contract Research Report No. 117/1996, Institute of Occupational Medicine, Edinburgh.
- Aitken, R. J., Baldwin, P. E. J., Beaumont, G. C., Kenny, L. C., & Maynard, A. D. (1999). Aerosol inhalability in low air movement environments. *Journal of Aerosol Science*, 30, 613–626.
- American Conference of Governmental Industrial Hygienists (1999a). *TLVs[®] and BEIs[®]*. Cincinnati, OH: ACGIH.
- American Conference of Governmental Industrial Hygienists (1999b). In J. H. Vincent (Ed.), *Particle size-selective sampling for particulate air contaminants*. Cincinnati, OH: ACGIH.
- Armbruster, L., & Breuer, H. (1982). Investigations into defining inhalable dust. In W. H. Walton (Ed.), *Inhaled particles V*. Oxford: Pergamon Press.
- Baldwin, P. E. J., & Maynard, A. D. (1998). A survey of windspeeds in indoor workplaces. *Annals of Occupational Hygiene*, 42, 303–313.
- Comité Européen de Normalisation (1993). *Workplace atmospheres: Size fraction definitions for measurement of airborne particles in the workplace. CEN Standard EN 481*. Brussels: CEN.
- CRC (1983). In R. C., Weast, & M. J. Astle (Eds.), *CRC handbook of chemistry and physics* (63rd ed.). Boca Raton, FL: CRC Press, Inc.
- Douglas, D. D. (1991). Respiratory protective devices. In G. D. Clayton, & F. E. Clayton (Eds.), *Patty's industrial hygiene and toxicology* (4th ed.), Vol. 1, Part A. New York: Wiley.
- Erdal, S., & Esmen, N. A. (1995). Human head model as an aerosol sampler: Calculation of aspiration efficiencies for coarse particles using an idealized human head model facing the wind. *Journal of Aerosol Science*, 26, 253–272.

- Hinds, W. C. (1999). *Aerosol technology: Properties, behavior, and measurement of airborne particles* (2nd ed.). New York: Wiley-Interscience.
- Hinds, W. C., & Kennedy, N. J. (2000). An ion generator for neutralizing concentrated aerosols. *Aerosol Science Techniques*, 32, 214–220.
- Hinds, W. C., & Kuo, T.-L. (1995). A low-velocity wind tunnel to evaluate inhalability and sampler performance for large dust particles. *Applied Occupational Environmental Hygiene*, 10, 549–556.
- International Standards Organization (1995). *Air quality—particle size fraction definitions for health-related sampling. ISO Standard 7708*. Geneva: ISO.
- International Commission on Radiological Protection (1994). In H. Smith (Ed.), *Human respiratory tract model for radiological protection, Annals of the ICRP, Publication 66*. Tarrytown, NY: Elsevier Science, Inc.
- Kuo, T.-L. (1993). *Inhalability evaluation of large dust particles using a full torso manikin*. Doctoral Dissertation, UCLA, Los Angeles.
- Mark, D., Vincent, J. H., Gibson, H., & Witherspoon, W. A. (1985). Applications of closely graded powders of fused alumina as test dusts for aerosol studies. *Journal of Aerosol Science*, 16, 125–131.
- Nelson, G. O., Johnson, R. E., Lindeken, C. L., & Taylor, R. D. (1972). Respirator cartridge efficiency studies III: A mechanical breathing machine to simulate human respiration. *American Industrial Hygiene Association Journal*, 33, 745–750.
- Ogden, T. L., & Birkett, J. L. (1977). The human head as a dust sampler. In W. H. Walton (Ed.), *Inhaled particles IV*. Oxford: Pergamon Press.
- Silverman, L. G., Plotkin, T., Sawyers, L. A., & Yancey, A. R. (1951). Air flow measurements on human subjects with and without respiratory resistance at several work rates. *Archives of Industrial Hygiene and Occupational Medicine*, 3, 461–478.
- Vincent, J. H. (1989). *Aerosol sampling: Science and practice*. Chichester, UK: Wiley.
- Vincent, J. H., & Mark, D. (1982). Application of blunt sampler theory to the definition and measurement of inhalable dust. In W. H. Walton (Ed.), *Inhaled particles V*. Oxford: Pergamon Press.
- Vincent, J. H., Mark, D., Miller, B. G., Armbruster, L., & Ogden, T. L. (1990). Aerosol inhalability at higher wind speeds. *Journal of Aerosol Science*, 21, 577–586.
- Vincent, J. H., Johnston, A. M., & Jones, A. D. (1984). The static electrification of airborne dusts in industrial workplaces. In B. Y. H. Liu, D. Y. H. Pui, & H. J. Fissan (Eds.), *Aerosols: Science, technology, and industrial applications of airborne particles*. Amsterdam, NY: Elsevier Science Publishing.